

Measurement of the ^{59}Co Quadrupole Moment by Observation of the Deformation Effect in the $^{59}\text{Co} + n$ Total Cross Section*

T. R. Fisher, A. R. Poletti, and B. A. Watson

Lockheed Palo Alto Research Laboratory, Palo Alto, California 94304

(Received 2 July 1973)

The deformation effect $\Delta\sigma_{\text{def}}$ in the $^{59}\text{Co} + n$ total cross section has been measured at neutron energies of 1.0, 1.2, 1.4, 1.6, 2.0, and 15.9 MeV employing a single-crystal target with 16% nuclear alignment. The average of the five measurements at energies between 1 and 2 MeV was $\Delta\sigma_{\text{def}} = -259 \pm 41$ mb; at 15.9 MeV, $\Delta\sigma_{\text{def}} = -87 \pm 42$ mb. These results, when interpreted using the first-order distorted-wave Born-approximation theory, imply a value of 0.39 ± 0.06 b for the quadrupole moment of ^{59}Co , which is in good agreement with the result of other techniques.

[NUCLEAR MOMENTS ^{59}Co ; measured deformation effect; deduced q , aligned ^{59}Co .]

I. INTRODUCTION

The difference in cross section between targets with and without nuclear alignment, designated the "deformation effect" $\Delta\sigma_{\text{def}}$, was first observed by Wagner, Miller, Tamura, and Marshak¹ in the $^{165}\text{Ho} + n$ total cross section. The effect is a result of the deformation of the nuclear matter distribution. Thus, information about the parameters of this distribution may be extracted if the nuclear-orientation parameters are known and if the reaction itself is understood. Deformation-effect studies can determine separately both the charge and mass quadrupole moments, including the sign. Alternative techniques can also provide this information but do not have the potential of aligned-target measurements for studying the detailed shape of the deformed nuclear matter distribution.

Several experimental observations of the deformation effect in ^{165}Ho have been made employing neutrons,¹⁻³ electrons,⁴ protons,⁵ and α particles⁶ as probes. Despite the formidable experimental difficulties, they have demonstrated the potential value of aligned-target measurements. In particular, the neutron total cross-section measurements have reinforced the interpretation of the "giant resonances" in neutron total cross sections first proposed by Peterson.⁷ The α -scattering measurements have aided in establishing a unique parametrization for the surface region of the α -nucleus optical potential.⁶ It seems desirable, then, to explore the possibilities of extending measurements of the deformation effect to nuclei other than ^{165}Ho . A logical candidate is ^{59}Co : Unlike ^{165}Ho , it is located in a region of the Periodic Table where rotational spectra, characteristic of large permanent nuclear deformations, are not found. Significant enhancements

of ground-state quadrupole moments over their single-particle values are observed but are attributed to coupling between the core and the odd nucleon which mixes excited vibrational states of the core into the ground-state wave function. Davies, Satchler, Drisko, and Bassel⁸ have pointed out that the deformation effect could be used to study the details of this coupling. Again, however, the simplest information which can be derived is the quadrupole moment of the nuclear matter distribution.

Alignment of ^{59}Co is more difficult than ^{165}Ho , since the hyperfine field is considerably weaker thus requiring that the target be operated at a much lower temperature. For example, at a temperature of 0.030 K, the nuclear alignment achievable by a thermal-equilibrium technique is still only 16% in magnetic fields of a few kilogauss. Continuous operation of targets at temperatures of 0.03 K or lower has been made possible by the development of the ^3He - ^4He dilution refrigerator. The heat which can be dissipated at these temperatures is small, however, and neutrons are therefore more attractive than charged-particle beams for use with such targets. Preliminary measurements employing a polycrystalline ^{59}Co target have been reported for neutron energies from 0.3 to 1.6 MeV.⁹ This paper reports measurements of the deformation effect in the $^{59}\text{Co} + n$ total cross section performed at energies of 1, 1.2, 1.4, 1.6, 2, and 15.9 MeV using a single-crystal target. The experimental arrangement is described in Sec. II. In Sec. III, calculations based on the distorted-wave Born-approximation (DWBA) theory of Ref. 8 are presented and used to extract a value of the quadrupole moment for comparison with the results of other techniques.

II. EXPERIMENTAL ARRANGEMENT

A. Experimental Geometry and Neutron Source

The experimental geometry for the neutron total cross-section measurements is shown in Fig. 1. Such measurements are frequently performed in open geometry, but the large mass of the cryostat necessitated some shielding to reduce the background from scattered neutrons. The paraffin collimators shown in Fig. 1 were sufficient to reduce the background to 3% of the transmitted neutron intensity at 1.5 MeV. The optimum sample length for measuring the total cross-section deformation effect has been discussed by Shelley¹⁰ and, in the present case, is approximately 5 cm. The cross-sectional area was limited by the availability of large cobalt single crystals and by the requirements for rapid cooling to 0.030 K. A cross-sectional area of 1 cm² was chosen, which gave a total sample mass of 45 g.

The requirements for sample size and shielding essentially fix the other parameters of the experimental geometry. Collimator and detector sizes were chosen so that the most efficient use was made of the available cross-sectional area of the sample. To reduce the effects of small changes in the position of the cobalt target, the cobalt was surrounded by a copper sheath which has a neutron transmission approximately equal to that of cobalt. All elements were carefully aligned along the beam axis using a transit, and the position of the cobalt target was checked when cold by substituting transparent Mylar windows for the stainless-steel windows normally used on the cryostat. The error introduced into the measured value of $\Delta\sigma_{\text{def}}$ by a sample misalignment of 1 mm was estimated to be less than 4% for the geometry of Fig. 1, and the probable misalignment of any element in Fig. 1 was less than 0.25 mm. The errors resulting from misalignment were, therefore, negligible in comparison with statistical uncertainties.

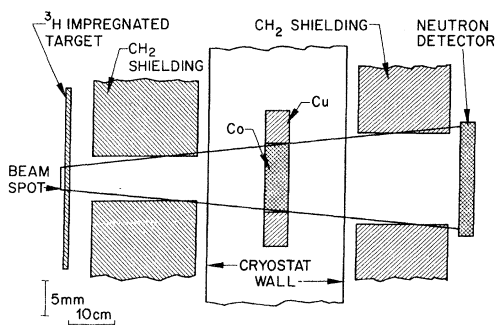


FIG. 1. Experimental geometry. Note the difference of a factor of 15 in the horizontal and vertical scales.

A tritium-impregnated titanium target 1 mg/cm² in areal density was bombarded by protons and deuterons from the Lockheed 3-MV Van de Graaff accelerator to produce neutron beams with average energies of 1, 1.2, 1.4, 1.6, 2, and 15.9 MeV. The typical energy spread was 100 keV at 1 MeV and 500 keV at 15.9 MeV. The transmitted neutrons were detected by a stilbene scintillation crystal operated in a γ -discrimination mode, and the neutron-source intensity was monitored by a paraffin-moderated BF₃ proportional counter positioned at an angle of 100° with respect to the beam.

B. Aligned ⁵⁹Co Target

It was first demonstrated by Grace *et al.*¹¹ that nuclear alignment occurs in cobalt single crystals at low temperatures, even in the absence of a magnetic field, and this fact has been used frequently in temperature measurements with activated cobalt crystals.¹² The atomic magnetic moments have a uniaxial alignment with respect to the "c" axis of the crystal and are coupled to the nuclear spin through the hyperfine interaction resulting in the nuclear alignment. In the present case, this feature simplified the design of the target because no external magnetic field was needed. Since the target was aligned but not polarized (no applied magnetic field), there was no possibility of a contribution from spin-spin effects, which have been observed to be large¹³ at these energies in ⁵⁹Co.

The ⁵⁹Co single-crystal target was prepared from five smaller crystals having the shape of cubes with a 1-cm edge. These cubes were cut from a larger rod so that the "c" axis was perpendicular to one face, then furnace brazed into a copper sleeve with Ag-Cu eutectic solder to form a rectangular solid 1 cm × 1 cm × 5 cm with the "c" axis parallel to the long dimension. The target was cooled by a ³He-⁴He dilution refrigerator system similar to that used previously for a polycrystalline ⁵⁹Co target.¹⁴ Starting from a temperature of 1 K, the time required to cool to 0.030 K, the lowest temperature achieved during the measurements of $\Delta\sigma_{\text{def}}$, was about 6 h. At this point, the target was still cooling but very slowly. The temperature of the target was measured by attaching a small activated ⁵⁹Co crystal and observing the anisotropy of the γ rays from the ⁶⁰Co decay. Small variations in temperature occurred during the course of the measurements of $\Delta\sigma_{\text{def}}$ since the target was actually cooling while data were being recorded, and these were monitored by Speer 220- Ω carbon resistors, grade 1002. The use of these resistors as temperature probes has been

discussed by Black, Roach, and Wheatley.¹⁵ It is possible to measure absolute temperatures to an accuracy of $\pm 2\%$ or better with a ^{60}Co thermometer¹⁶; in the present case, an error of $\pm 10\%$ was allowed, primarily because of the large size of the cobalt target and the possibility that it was not in complete thermal equilibrium with the thermometer.

The nuclear alignment in the cobalt target can be calculated from the temperature and the known strength of the hyperfine coupling. From NMR measurements, the hyperfine field at 0 K in cobalt metal is 222 kOe,¹⁷ and the nuclear magnetic moment of ^{59}Co is $4.616\mu_N$ ¹⁸ leading to the value 1.07×10^{-2} K for the hyperfine parameter $H\mu/kI$. The calculated nuclear alignment $B_2/B_2(\text{max})$ at 0.030 ± 0.003 K is then $15.9 \pm 2.3\%$, if the "c" axis of the crystal or, equivalently, the neutron beam direction, is chosen as the Z axis.

C. Recording and Analysis of Data

The procedure for the recording and analysis of data followed that employed in previous measurements on ^{165}Ho .² At each energy, the difference in transmission through the ^{59}Co target was observed for target temperatures of approximately 0.030 and 0.300 K. A typical measurement is illustrated in Fig. 2. The detector spectra were stored on magnetic tape so that corrections for gain shifts could be made in the analysis, but such corrections proved to be negligible. During the course of several days, the gain stability of both detectors was better than 0.5% and the effects of gain shifts were further reduced by the procedure

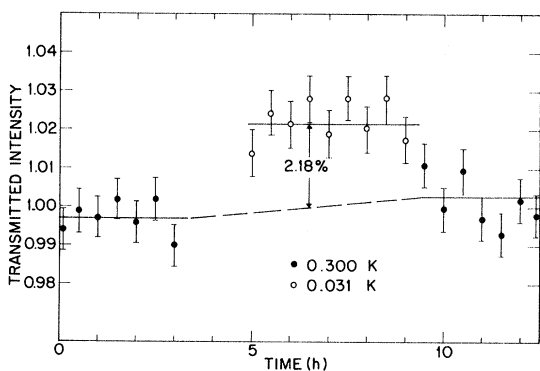


FIG. 2. Typical measurement of $\Delta\sigma_{\text{def}}$ at a neutron energy of 1 MeV. The ordinate shows the transmitted neutron intensity which has been normalized to an average of unity for the warm-target runs. The points show the statistical consistency of the data when read out at intervals of approximately one half hour. The difference between the average of the cold and warm runs is 2.18% corresponding to $\Delta\sigma_{\text{def}} = -346$ mb for 100% alignment.

of alternating warm and cold runs.

If $\Delta T/T$ is the change in sample transmission between the warm and cold runs, then for $\Delta T/T \ll 1$

$$\Delta\sigma_{\text{def}} \approx \frac{1}{N_s l} \frac{\Delta T}{T} \frac{B_2(\text{max})}{B_2} (1+C), \quad (1)$$

where N_s is the number of nuclei per unit volume and l is the sample length. The first-order DWBA theory predicts that the deformation effect actually observed will be proportional to the nuclear alignment B_2 , and this assumption has been used in Eq. (1) to normalize $\Delta\sigma_{\text{def}}$ to correspond to 100% alignment. The factor $(1+C)$ is a correction for neutrons which reach the detector after small-angle scattering in the ^{59}Co target (inscattering) or after scattering from other parts of the apparatus (background). In the present case, this factor was 1.035 ± 0.02 . The procedures for its evaluation are discussed in Refs. 10 and 19.

The final results for $\Delta\sigma_{\text{def}}$ are shown in Fig. 3. The single point at 1.5-MeV energy represents an average of the five individual measurements shown in the insert. Energy averaging is essential to remove possible effects of individual compound-nuclear resonances. The curves in Fig. 3 were calculated using the first-order DWBA theory which is described in the next section.

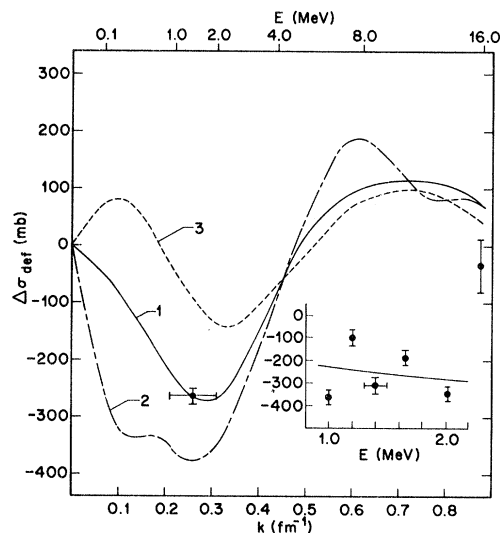


FIG. 3. Summary of results for $\Delta\sigma_{\text{def}}$. The five measurements shown in the insert are averaged and presented as a single point with an average energy of 1.5 MeV and an energy spread of 1 MeV for comparison with the DWBA calculation. The three curves were calculated for different sets of optical parameters using the form of Eq. (3) for $F_2(r)$ and a strength $A_2 = 44$ MeV. The optical parameters used in the calculation are given in Table I. Curve 1 corresponds to the "best" optical parameters as determined by fitting available data on the $^{59}\text{Co} + n$ cross section.

III. RESULTS

A. First-Order DWBA Calculation

We assume that the interaction between the neutron and the ^{59}Co nucleus is described by a deformation deformation effect:

$$\Delta\sigma_{\text{def}} = \left(\frac{4\pi}{5}\right)^{1/2} \frac{1}{kE} \text{Im} \sum_{\substack{LL' \\ JJ'}} (i)^{L-L'} (2J+1)(2J'+1) \left(J\frac{1}{2} - \frac{1}{2} \mid L0\right) \left(J'\frac{1}{2} - \frac{1}{2} \mid L'0\right) \\ \times \left(J\frac{1}{2} J' - \frac{1}{2} \mid 20\right)^2 \int \chi_{L'J'}(r) \chi_{LJ}(r) A_2 F_2(r) dr. \quad (2)$$

The χ 's are the distorted radial wave functions corresponding to orbital angular momentum L and total angular momentum J , and the quantity $A_2 F_2(r)$ is derived from the deformed part of the optical potential. It is this quantity, written here as the product of a strength and form factor, which is actually determined by aligned-target measurements. In general, higher-order terms such as $A_4 F_4(r)$, corresponding to a hexadecapole deformation, etc., may also contribute to $\Delta\sigma_{\text{def}}$, but their contribution is generally small in comparison with the quadrupole term and in the present analysis they have been neglected. The effect of a hexadecapole deformation would have been unobservable in the present experiment in any case because of the small value of B_4 [$B_4/B_4(\text{max}) \approx 0.006$].

In principle, detailed measurements of the deformation effect in the differential cross section as well as the total cross section could uniquely determine both the strength and form factor of the deformed potential. However, the total cross-section measurement above is insufficient for this purpose, and it is necessary to make some assumption concerning the form factor $F_2(r)$. Both the vibrational and rotational models give the same prediction, to first order, for $F_2(r)$,⁸ namely

$$F_2(r) = \frac{d}{dx} (1 + e^x)^{-1}, \quad (3) \\ x = \frac{r - R_a}{a},$$

if the usual Woods-Saxon form is assumed for the real part of the optical potential. Measurements of $\Delta\sigma_{\text{def}}$ then serve to fix the value of the strength A_2 , which may be expressed in terms of the parameters of either the vibrational or rotational model. If it is additionally assumed that the neutron and proton densities are the same and are proportional to the form factor for the real part of the optical potential, $(1 + e^x)^{-1}$, A_2 is related to the quadrupole moment Q by

$$Q = -\frac{6ZR_a a}{5U} \frac{5}{4\pi} (II20 \mid II) A_2, \quad (4)$$

formed optical potential. If the deformation is small, its effect on the cross section may be calculated using the first-order DWBA theory given in Ref. 8. From the expressions found there together with the optical theorem, we can derive the following expression for the total cross-section

where U is the strength of the real part of the optical potential and R_a is the radius. As defined in Eq. (4), Q is the observable quadrupole moment rather than the intrinsic quadrupole moment, Q_0 , of the rotational model, and Eq. (4) is applicable to either the vibrational or rotational picture.

The radial distorted waves χ_{LJ} were generated using an optical potential of the form

$$V(r) = -Uf(r) - iWg(r) + V_{\text{so}} \frac{\lambda_{\pi}^2}{r} \frac{df}{dr} \vec{\sigma} \cdot \vec{1}, \\ f(r) = (1 + e^{(r-R_a)/a})^{-1}, \quad (5) \\ g(r) = e^{-[(r-R_b)/b]^2}.$$

This potential was chosen because it has been successfully employed by Moldauer²⁰ to fit a large amount of low-energy neutron scattering data in this mass region. The best values of the optical parameters were selected by minimizing χ^2 for the fit to neutron total cross-section data at 0.5, 1, 4, 8, and 14 MeV²¹ and differential cross-section data at 1, 4, and 14 MeV.²² When the consensus parameters of Ref. 20 were used as a starting point and parameters U , W , R_a , and R_b were allowed to vary, the minimum χ^2 occurred for the parameter set shown in column 2 of Table I. The energy dependence of the real potential was fixed arbitrarily as $-0.3E$ since it has been established that local potentials have an energy dependence of about this magnitude.²³

The calculation of $\Delta\sigma_{\text{def}}$ employing the above optical parameters is shown in Fig. 3 for $A_2 = 44.7$ MeV, or $Q = 0.39$ b. Curves are also shown for two additional sets of optical parameters: a set derived by Perey²³ primarily from fits to proton scattering data and a set derived by Marshak *et al.*³ from fits to neutron total cross-section measurements on cadmium and lead. These parameter sets are given in columns 3 and 4 of Table I. Although the calculated curves for $\Delta\sigma_{\text{def}}$ are qualitatively similar, the choice of optical parameters clearly affects the value of A_2 (or Q) extracted from the data and should be made as carefully as possible.

TABLE I. Optical parameters used in the calculation of the theoretical curves of Fig. 3.

| | Best fit to ^{59}Co data | Perey (Ref. 23) | Marshak <i>et al.</i> (Ref. 3) |
|----------|--------------------------------------|-----------------------|-----------------------------------|
| U | 48–0.3E MeV | 51–0.55E MeV | 47.3–0.23E MeV |
| W | 14.47 MeV | 13.5 MeV ^a | 4.28–0.41E ^a |
| R_a | 4.86 fm | 4.88 fm | 4.70 fm |
| R_b | 5.55 fm | 4.88 fm | 4.70 fm |
| a | 0.62 fm | 0.65 fm | 0.68 fm |
| b | 0.47 fm | 0.47 fm | 0.64 fm |
| V_{so} | 7.0 MeV | 7.5 MeV | 7.0 MeV |
| χ^2 | 73 | 475 | 274 |

^a Derivative Woods-Saxon shape.

B. ^{59}Co Quadrupole Moment

The five measurements of $\Delta\sigma_{\text{def}}$ at energies between 1 and 2 MeV show a scatter which is significantly greater than the statistical uncertainty (see Fig. 3, insert) and is presumably due to the structure which is present in the total cross section. These five measurements were averaged for purposes of comparison with results of the DWBA calculation. The best value of A_2 , the deformed potential strength, was determined from this average together with the 15.9-MeV point using inverse-square weighting. The resulting statistical uncertainty of 6.2% was combined with an uncertainty of 14.4% in $B_2/B_2(\text{max})$ to give the result $A_2 = 44.0 \pm 7.1$ MeV. Subject to the validity of Eq. (4), this implies $Q = 0.39 \pm 0.06$ b.

In Table II, the present result is compared with other measurements of the ^{59}Co quadrupole moment. The agreement with previous measurements employing atomic spectroscopy and photonuclear cross-section techniques is good and the accuracy of the present result is comparable to that of the other techniques. The precision of the present result could be improved by a more accurate determination of $B_2/B_2(\text{max})$ for the ^{59}Co target. It would also be desirable to improve the calculation of $\Delta\sigma_{\text{def}}$, either by carrying the DWBA calculation out to second order or by employing the coupled-channel formalism. The error which results from neglecting higher-order terms in the DWBA calculation is not known, but could well

TABLE II. Measurements of the ground-state quadrupole moment of ^{59}Co .

| Method | Q (b) |
|---|-----------------|
| Atomic spectroscopy ^a | 0.50 ± 0.20 |
| Atomic spectroscopy ^b | 0.40 ± 0.04 |
| Photonuclear cross section ^c | 0.44 ± 0.06 |
| Photonuclear cross section ^d | 0.40 ± 0.06 |
| Neutron aligned-target cross section ^e | 0.39 ± 0.06 |

^a K. Murakawa and T. Kamei, Phys. Rev. 92, 325 (1953).

^b D. V. Ehrenstein, H. Kopfermann, and S. Penselin, Z. Phys. 159, 230 (1960).

^c S. C. Fultz, R. L. Bramblett, J. T. Caldwell, N. E. Hansen, and C. P. Jupiter, Phys. Rev. 128, 2345 (1962).

^d G. Baciu, G. C. Bonazzola, B. Minetti, C. Molino, L. Pasqualini, and G. Pirogino, Nucl. Phys. 67, 178 (1965).

^e Present experiment.

be as large as 10 or 15%.

The present result of $\Delta\sigma_{\text{def}} = -259 \pm 41$ mb obtained for the average over the energy region from 1 to 2 MeV differs somewhat from the previous result obtained with a polycrystalline ^{59}Co target. If we take the measurements at 1, 1.15, 1.4, and 1.63 MeV from Ref. 9, average them, and divide by the quoted value of $B_2/B_2(\text{max})$, we obtain $\Delta\sigma_{\text{def}} = -400 \pm 100$ mb. Although the two results are statistically consistent, the present result is considered to be more reliable since the single-crystal target had no net polarization, thus no possible contribution from a spin-spin effect. We have, therefore, preferred not to take a weighted average of the two results, but have relied solely on the present data to extract the value of Q .

It is concluded that, in favorable cases, the technique of neutron cross-section measurements on aligned targets may be used to obtain an accurate measurement of a nuclear quadrupole moment. As previously mentioned, however, it seems of greater interest to apply the technique to study the form factor $F_2(r)$ of the deformed part of the interaction potential. This would require differential cross-section measurements which are feasible, although they are considerably more difficult than the total cross-section measurements presented here.

*Work supported by the Lockheed Independent Research Fund.

¹R. Wagner, P. D. Miller, T. Tamura, and H. Marshak, Phys. Rev. 139, B29 (1965).

²T. R. Fisher, R. S. Safrata, E. G. Shelley, J. McCarthy, and S. M. Austin, Phys. Rev. 157, 1149 (1967); J. S. McCarthy, T. R. Fisher, E. G. Shelley, R. S. Safrata,

and D. Healey, Phys. Rev. Lett. 20, 502 (1968).

³H. Marshak, A. Langsford, T. Tamura, and C. Y. Wong, Phys. Rev. C 2, 1862 (1970).

⁴R. S. Safrata, J. S. McCarthy, W. A. Little, M. R. Yearian, and R. Hofstadter, Phys. Rev. Lett. 18, 667 (1967); F. J. Urhane, J. S. McCarthy, and M. R. Yearian, *ibid.* 26, 578 (1971).

- ⁵T. R. Fisher, S. L. Tabor, and B. A. Watson, *Phys. Rev. Lett.* **27**, 1078 (1971).
- ⁶D. R. Parks, S. L. Tabor, B. B. Triplett, H. T. King, T. R. Fisher, and B. A. Watson, *Phys. Rev. Lett.* **29**, 1264 (1972).
- ⁷J. W. Peterson, *Phys. Rev.* **125**, 955 (1962).
- ⁸K. T. R. Davies, G. R. Satchler, R. M. Drisko, and R. H. Bassel, *Nucl. Phys.* **44**, 604 (1963).
- ⁹T. R. Fisher, D. C. Healey, J. S. McCarthy, and D. Parks, in *Proceedings of the Third International Symposium on Polarization Phenomena in Nuclear Reactions, Madison, 1970*, edited by H. H. Barschall and W. Haeberli (Univ. of Wisconsin Press, Madison, Wisc., 1971), p. 641.
- ¹⁰E. G. Shelley, Ph. D. thesis, Stanford University, 1966 (unpublished).
- ¹¹M. A. Grace, C. E. Johnson, N. Kurti, R. G. Scurlock, and R. T. Taylor, *Philos. Mag.* **4**, 948 (1959).
- ¹²See, for example, T. L. Thorp, B. B. Triplett, W. D. Brewer, N. E. Phillips, D. A. Shirley, J. E. Templeton, R. W. Stark, and P. H. Schmidt, *J. Low Temp. Phys.* **3**, 589 (1970).
- ¹³T. R. Fisher, H. A. Grench, D. C. Healey, J. S. McCarthy, D. Parks, and R. Whitney, *Nucl. Phys. A179*, 241 (1972).
- ¹⁴T. R. Fisher, D. C. Healey, D. Parks, S. Lazarus, J. S. McCarthy, and R. Whitney, *Rev. Sci. Instrum.* **41**, 684 (1970).
- ¹⁵W. C. Black, Jr., W. R. Roach, and J. C. Wheatley, *Rev. Sci. Instrum.* **35**, 587 (1964).
- ¹⁶H. Marshak, private communication.
- ¹⁷H. Yasuoka and R. T. Lewis, *Phys. Rev.* **183**, 559 (1969).
- ¹⁸D. A. Shirley, in *Hyperfine Structure and Nuclear Radiations*, edited by D. A. Shirley and E. Matthias (North-Holland, Amsterdam, 1968), p. 985.
- ¹⁹D. C. Healey, Ph. D. thesis, Stanford University, 1970 (unpublished).
- ²⁰P. A. Moldauer, *Nucl. Phys.* **47**, 65 (1963).
- ²¹*Neutron Cross Sections*, compiled by M. D. Goldberg, S. F. Mughabghab, S. N. Purohit, B. A. Magurno, and V. M. May, Brookhaven National Laboratory Report No. BNL-325 (U.S. GPO, Washington, D.C., 1966), 2nd ed., 2nd Suppl., Vol. IIa, Z-21 to 40.
- ²²M. Walt and H. H. Barschall, *Phys. Rev.* **93**, 1062 (1954); G. V. Gorlov, N. S. Lebedeva, and V. M. Morosov, *Phys. Lett.* **25B**, 197 (1967); C. St. Pierre, M. K. Machwe, and P. Lorrain, *Phys. Rev.* **115**, 999 (1959); *Neutron Cross Sections* (see Ref. 21).
- ²³F. G. Perey, *Phys. Rev.* **131**, 745 (1963).